Theor Chem Acc (2004) 112: 95–105
DOI 10.1007/s00214-004-0570-7

Theoretical
Chemistry Accounts

Regular article

Ab initio study of the oxidation of CH_3SH to CH_3SSCH_3

Rois Benassi

Dipartimento di Chimica, Università di Modena e Reggio E., Via Campi 183, 41100, Modena, Italy

Received: 12 May 2003 / Accepted: 13 June 2003 / Published online: 8 April 2004
© Springer-Verlag 2004

Abstract. The thermodynamic and kinetic aspects of the oxidation of methanethiol to dimethyl disulfide by oxygen were studied using ab-initio molecular techniques. The reaction was considered as a multi-step process. Geometrical parameters and molecular energies for critical points were determined and characterized at the MP2(Full)/6–31G* level. Afterwards, a study was carried out employing different methods of theoretical model chemistry (G2, G2(MP2), G3 and CBS-4 MB), for which the equilibrium geometry at MP2(Full)/6–31G* was assumed as starting point. The steps governing the rate of the whole reaction were determined and prove to be the same for any level of theory employed. Although the MP2(Full)/6–31G* level is able to afford a good qualitative description of the reaction pathway, the quantitative aspect is less satisfactory. Results from the methods of theoretical model chemistry, on the other hand, accord well with experimental data, if available, and are very useful for studying the thermodynamic and kinetic aspects of chemical reactions.

Keywords: Sulfur oxidation – Model chemistry – Ab-initio molecular orbital methods – Reaction pathway

1. Introduction

Oxidation reactions of organic sulfides are of great importance in biological systems [1, 2], both in the atmosphere [3] and on surfaces [4].The sulfur atom can bind one or more oxygen atoms, but the first step, for ordinary oxidation, is the formation of a disulfide molecule. The formation of the disulfide bond is governed by an ox–redox equilibrium and is very important in determining the structure of the proteins [5].The oxidation of pure thiols with molecular oxygen at low temperatures is an extremely slow reaction. In the presence of basic catalysts and/or olefins, however, thiol oxidation by air proceeds rapidly. Such oxidations are commonly used for conversion, by air, of thiols to disulfides, according to the overall reaction:

$$RSH + 1/2O_2 \rightarrow RSSR + H_2O \qquad (1)$$

The proposed [6, 7] course of this reaction is a multistep process. As with the air-oxidation of carbanions, formation of a thiolate anion is believed to be the initial step of the reaction. This is a reversible step with a basic catalyst:

$$RSH + OH^- \rightleftarrows RS^- + H_2O \qquad (2)$$

In the next step the anion reacts with oxygen via electron transfer to give the thiyl radical and peroxide ion:

$$RS^- + O_2 \rightleftarrows RS^{\cdot} + O_2^{-\cdot} \qquad (3)$$

Dimerization of the thiyl radical leads to disulfide:

$$2RS^{\cdot} \rightarrow RSSR \qquad (4)$$

The peroxide ion formed in Eq. (3) can also oxidize the thiol as indicated below:

$$RSH + O_2^{-\cdot} \rightarrow RS^{\cdot} + HO_2^- \qquad (5)$$

$$RSH + HO_2^- \rightarrow RS^{\cdot} + OH^- + OH^{\cdot} \qquad (6)$$

Electronic Supplementary Material Supplementary material, a table of Cartesian co-ordinates at MP2(Full)/6–31g* for each molecule and complex studied, is available in the online version of this article at http://dx.doi.org/10.1007/s00214-004-0570-7

Correspondence to: Rois Benassi
e-mail: benassi.rois@unimore.it

Table 1. Comparison of calculated and experimental heats of reaction[a] (standard deviations are reported in parentheses)

Reaction	Experimental[b]	6–31G*MP2(Full)	G2	G2(MP2)	G3	CBS-4 MB
2	−33.80	−59.16 (−25.36)	−32.09 (1.71)	−32.07 (1.73)	−34.06 (−0.26)	−28.72 (5.08)
3	34.00	34.79 (0.79)	32.52 (−1.48)	33.67 (−0.33)	33.94 (−0.06)	29.23 (−4.77)
4	−65.40	−53.07 (12.33)	−64.56 (0.84)	−66.50 (−1.10)	−63.07 (2.33)	−63.60 (1.80)
5	22.80	32.30 (9.50)	21.35 (−1.45)	20.78 (−2.02)	21.36 (−1.44)	26.82 (4.02)
6	34.50	43.04 (8.54)	32.46 (−2.04)	32.92 (−1.58)	30.94 (−3.56)	29.39 (−5.11)
7	−31.90	−32.55 (−0.65)	−32.17 (−0.27)	−32.17 (−0.27)	−32.01 (−0.11)	−31.59 (0.31)
1/2(2 + 3 + 2×4 + 5 + 6 + 7)	−52.60	−39.47 (13.13)	−53.53 (−0.93)	−54.94 (−2.34)	−52.99 (0.30)	−51.03 (1.56)

[a] kcal mol^{-1}
[b] Ref. [21]

$$RSH + OH^{\cdot} \rightarrow RS^{\cdot} + H_2O \qquad (7)$$

The sum of all these reactions gives the global reaction represented by Eq. (1). The basic catalyst promotes thiolate anion formation and consequently the overall reaction.

The aim of the present work is to analyse the thermodynamic and kinetic aspects of each single reaction. The thermodynamic properties are derived by ab-initio calculation at different theory levels. At the first level, the ab-initio calculations were performed employing the 6–31G* basis set and second-order Møller–Plesset perturbation theory MP2. Thermodynamic properties were obtained by complete vibrational analysis. Afterwards, a study was carried out employing different methods of theoretical chemistry. These methodologies, developed to obtain thermochemical properties with a high degree of accuracy, were also applied to obtain information on the reactive potential energy surfaces [8, 9, 10, 11].

2. Computational Method

All calculations were performed with the Gaussian 94 [12] and Gaussian 98 [13] program packages, run on

Table 2. Molecular energy differences ΔE (without ZPE correction), $\Delta E(0)$ (with ZPE correction), and thermodynamic properties (ΔH, ΔG, and ΔS) with respect to the transition state for the reaction $CH_3SH + OH^- \rightleftarrows CH_3S^- + H_2O$. Arrhenius parameters ($E_a$, log k, and log A) at 298.15 K

	ΔE[a]	$\Delta E(0)$[a]	ΔH[a]	ΔG[a]	ΔS[b]	E_a	log k[c]	log A[c]
MP2(Full)/6–31G*								
$CH_3SH + OH^-$	20.88	20.05	20.89	11.95	30.02			
C1	−0.73	−0.28	0.08	−0.58	2.23			
TS	0.00	0.00	0.00	0.00	0.00	0.51	16.79	17.16
C2	−58.02	−55.11	−54.71	−56.46	5.88			
$CH_3S^- + H_2O$	−39.98	−39.07	−38.27	−47.67	31.53			
G2								
$CH_3SH + OH^-$	6.61	5.78	6.623	−2.32	30.02			
C1	−0.42	0.03	0.40	−0.26	2.23			
TS	0.00	0.00	0.00	0.00	0.00	0.19	17.02	17.16
C2	−42.38	−39.48	−39.08	−40.83	5.88			
$CH_3S^- + H_2O$	−27.18	−26.27	−25.47	−34.87	31.53			
G2(MP2)								
$CH_3SH + OH^-$	6.57	5.74	6.59	−2.36	30.02			
C1	−0.42	0.03	0.39	−0.27	2.23			
TS	0.00	0.00	0.00	0.00	0.00	0.20	17.01	17.16
C2	−42.41	−39.51	−39.11	−40.86	5.88			
$CH_3S^- + H_2O$	−27.20	−26.29	−25.49	−34.89	31.53			
G3								
$CH_3SH + OH^-$	9.45	8.62	9.46	0.51	30.02			
C1	0.96	1.41	1.77	1.11	2.23			
TS	0.00	0.00	0.00	0.00	0.00	−1.18	18.02	17.16
C2	−41.82	−38.92	−38.52	−40.27	5.88			
$CH_3S^- + H_2O$	−26.31	−25.41	−24.61	−34.01	31.53			
CBS-4 MB								
$CH_3SH + OH^-$	5.64	4.81	5.65	−3.30	30.02			
C1	1.77	2.22	2.59	1.93	2.23			
TS	−0.00	0.00	−0.00	0.00	0.00	−2.00	18.62	17.16
C2	−40.70	−37.80	−37.40	−39.15	5.88			
$CH_3S^- + H_2O$	−24.78	−23.87	−23.07	−32.47	31.53			

[a] kcal mol^{-1}
[b] cal mol^{-1}
[c] cm^3 mol^{-1} s^{-1}

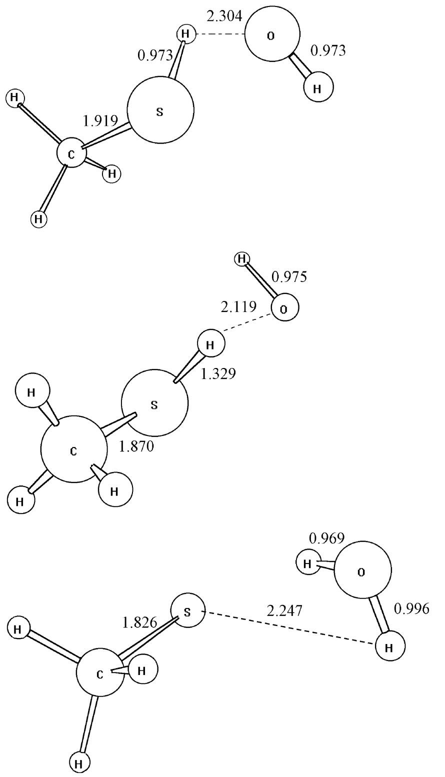

Fig. 1. Features of the optimized MP2(Full)/6-31G* geometries of C1, TS, and C2 for Eq. (2). Distances in Å

different computers (Silicon Graphics 4CPU MIPS R10000 unit, IBM RS/6600 workstation and Origin 2000). At the first level (of approach), the electronic properties were obtained with the 6–31G* basis set, and correlation effects were calculated with the frozen MP2(Fc) treatment. UHF wave functions were employed for the open-shell systems and spin-projection operators were applied to remove contamination for higher spin states (PMP2). Geometry optimizations were carried out on all reactants, products, and transition states and then harmonic frequencies were calculated. Zero-point energies and thermal corrections to 298 K were determined using a scale factor of 0.9434 for frequency. The presence of one normal mode of imaginary frequency confirmed the identity of the transition state. Analysis of the reaction path also revealed the formation of intramolecular complexes, which prove to be minimum energy points.

The total energy for all species was then calculated using different model chemistry schemes. The complete basis set method CBS-4 M [14] was employed in the modified version, CBS-4 MB [15], which was proposed for application to molecules of increasing molecular size, including organic sulfur derivatives. The other methodologies used were G2 [16], G2(MP2) [17], and G3 [18]. The two initial steps for all these methods are the determination of an initial geometry (at the 3–21g* level for CBS and the 6–31G* level for G), after which harmonic frequencies are calculated and scaled to give zero-point energy and thermal corrections. In a few of the reactions studied, neither of these basis sets (3–21g* and 6–31G* without the inclusion of the correlation effects at MP2 level) enabled us to characterize the intramolecular complexes as minimum energy points on the energy hypersurface or, rather more importantly, the transition state, as previously found at the 6–31*/MP2 level. These results suggested that changes should be made to the scheme of compound methods. Since, in the G schemes, the geometry is refined at the MP2(Full)/6–31G* level and this geometry is then used for a series of single-point calculations in the subsequent steps, the first two steps for both the compound methods (CBS and G) were changed as follows:

1. geometry was calculated at the MP2(Full)/6–31G* level; and
2. harmonic frequencies were calculated at the MP2(Fc)/6–31G* level (in order to save computational time) and scaled with a factor of 0.9434.

All the results here reported were then referred to the same molecular geometry MP2(Full)/6–31G* and zero-point energy, together with the thermal corrections at 298 K at the MP2(Fc)/6–31G* level.

Activation energies of reactions were calculated using conventional transition state theory [19] from data obtained at the different levels of theory. Tunnelling corrections [20] are included.

3. Heat of reaction

The experimental and calculated heats for the total reaction (Eq. 1) and for each single-step reaction (Eqs. 2, 3, 4, 5, 6, and 7) are reported in Table 1. The comparison between experimental and calculated values can provide a check on the validity of the application for each single method of calculation employed. All the methods predict a global exothermic process. The simplest approach (MP2(Full)/6–31G*) is the one that affords values notably different from the experimental value (13.13 kcal mol^{-1}). All the compound methods provide enthalpies of reaction very close to experimental values with an accuracy (except for G2(MP2)) that falls within the tolerances of model chemistry (1–2 kcal mol^{-1}). The G3 scheme yields the smallest error (0.30 kcal mol^{-1}), but CBS-4 MB (faster and less expensive in terms of calculation resources) also works rather well (1.56 kcal mol^{-1}). It was found that all the methodologies employed enabled the thermochemistry of a reaction to be studied with a good degree of accuracy. The analysis of the data for each single step (Eqs. 2, 3, 4, 5, 6, and 7) leads to the same conclusions. In the employment of the compound methods it must be remembered that the enthalpies of formation for each single molecular species could include the accumulation of small errors [15, 22], especially for large molecules. In the calculations of the enthalpies of reaction, these errors could annul one another or accumulate. Consequently, the values obtained for these quantities must be tested with care, keeping in mind that, although they could attest qualitatively to the

Table 3. Molecular energy differences ΔE (without ZPE correction), $\Delta E(0)$ (with ZPE correction), and thermodynamic properties (ΔH, ΔG and ΔS) with respect to the transition state for the reaction $CH_3S^- + O_2 \rightleftarrows CH_3S^{\cdot} + O_2^{-\cdot}$. Arrhenius parameters ($E_a$, log k, and log A) at 298.15 K

	ΔE^a	$\Delta E(0)^a$	ΔH^a	ΔG^a	ΔS^b	E_a	log k^c	log A^c
MP2(Full)/6–31G*								
$CH_3S^- + {}^3O_2$	−26.55	−27.54	−26.96	−36.65	32.50	(27.55	−9.58	10.61)^d
$CH_3S^- + {}^1O_2$	8.50	7.24	7.83	−1.25	30.43			
C1	−0.07	1.91	1.98	1.92	0.19			
TS	0.00	0.00	0.00	0.00	0.00	−1.38	18.69	17.67
C2	−12.14	−11.24	−10.94	−11.76	2.72			
$CH_3S^{\cdot} + O_2^-$	17.56	15.93	16.60	6.51	33.85			
G2								
$CH_3S^- + {}^3O_2$	−22.67	−23.66	−23.08	−32.77	32.50	(23.67	−6.74	10.61)^d
$CH_3S^- + {}^1O_2$	4.50	3.24	3.83	−5.25	30.43			
C1	2.86	4.84	4.91	4.85	0.19			
TS	0.00	0.000	0.00	0.00	0.00	−4.31	20.84	17.67
C2	−18.66	−17.77	−17.47	−18.28	2.72			
$CH_3S^{\cdot} + O_2^-$	10.40	8.77	9.44	−0.65	33.85			
G2(MP2)								
$CH_3S^- + {}^3O_2$	−23.25	−24.24	−23.66	−33.35	32.50	(24.25	−7.16	10.61)^d
$CH_3S^- + {}^1O_2$	3.40	2.14	2.73	−6.35	30.43			
C1	3.00	4.97	5.04	4.98	0.19			
TS	0.00	0.00	0.00	0.00	0.00	−4.45	20.93	17.67
C2	−19.51	−18.61	−18.31	−19.13	2.72			
$CH_3S^{\cdot} + O_2^-$	10.97	9.33	10.00	−0.09	33.85			
G3								
$CH_3S^- + {}^3O_2$	−23.99	−24.98	−24.41	−34.10	32.50	(25.00	−7.71	10.61)^d
$CH_3S^- + {}^1O_2$	5.54	4.28	4.86	−4.21	30.43			
C1	2.94	4.92	4.99	4.93	0.19			
TS	0.00	0.00	0.00	0.00	0.00	−4.39	20.89	17.67
C2	−17.29	−16.40	−16.10	−16.91	2.72			
$CH_3S^{\cdot} + O_2^-$	10.50	8.86	9.54	−0.56	33.85			
CBS-4 MB								
$CH_3S^- + {}^3O_2$	−33.47	−34.45	−33.89	−43.57	32.50	34.48	−14.66	10.61
$CH_3S^- + {}^1O_2$	1.32	0.06	0.64	−8.43	30.43			
C1	5.14	7.12	7.18	7.13	0.19			
TS	0.00	0.00	0.00	0.00	0.00	−6.59	22.51	17.67
C2	−20.19	−21.09	−20.79	−21.60	2.72			
$CH_3S^{\cdot} + O_2^-$	−6.97	−5.33	−4.66	−14.75	33.85			

[a] kcal mol^{-1}
[b] cal mol^{-1}
[c] cm^3 mol^{-1} s^{-1}
[d] Considering this point as starting point

endothermic or exothermic character of reaction, quantitatively they could be unsatisfactory. These complications should not exist in the calculations reported here: not only was the molecular size not overly large, but the version CSB-4 MB employed was developed specifically to minimize the problem [15].

The whole process turns out to be exothermic, but the total value for enthalpy of reaction derives from the sum of the single steps represented by Eqs. 2, 3, 4, 5, 6, and 7. Some steps are exothermic (Eqs. 2, 4, and 7), others endothermic (Eqs. 3, 5, and 6). The latter are those that would appear to control the course of the reaction. In order to examine more accurately the mechanism and the kinetics of the reaction, each single step has been studied in detail.

$CH_3SH + OH^- \rightleftarrows CH_3S^- + H_2O$

Methyl thiol is acid enough (p K_a 10.3 [23]) to form salts even with weak bases. Thiolate anion formation, the starting step for the proposed mechanism, is relatively easy and greatly influenced by the basic catalyst. Scanning the energy hypersurface at MP2(Full)/6–31G* level, a transition state (TS) was located. Frequency analysis (MP2(Fc)/6–31G*) showed that this state is a first-order saddle-point, with a single mode with an imaginary frequency. According to the adopted scheme of calculation, this structure remains the same for all the methods employed. The value of the differences of the molecular energies and the thermodynamic properties with respect to the TS obtained with the different approaches are reported in Table 2. If the initial energy ground state for the reaction is considered as the sum of the energies of the single reactants, the TS lies in a minimum of the energy hypersurface. This suggests the presence of an energy minimum that could result from the formation of a molecular complex in the entrance channel of the reaction. The importance of the formation of intramolecular complexes (van der Waals species) to the overall reaction mechanism has been already

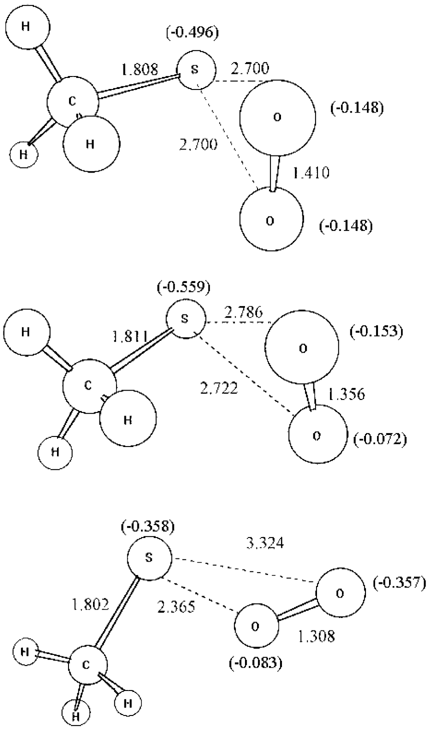

Fig. 2. Features of the optimized MP2(Full)/6-31G* geometries of C1, TS and C2 for Eq. (3). Distances in Å. Atomic charges from NBO population analysis

pointed out [24, 25] and demonstrated, for example in the oxidation of disulfides [26]. In order to examine this question, an IRC [27] calculation was performed along the reaction co-ordinate at the MP2(Fc)/6–31G* level. Two energy minimum values, backwards and forwards with respect to the TS, are found, which are lower than those of the products and reagents. A full optimization at MP2(Full)/6–31G* level characterized these two points as minima along the reaction path, as confirmed by a complete frequency analysis. The structures of these two complexes, namely, C1 for the entrance and C2 for the exit reaction channel, is illustrated in Fig. 1.

The difference in total electronic energy (MP2(Full)/6–31G* level) is very small for the C1 complex (−0.73 kcal mol^{-1}) and subsequently reduces with the inclusion of ZPE correction (−0.28 kcal mol^{-1}). The ΔG is also small and negative (−0.58 kcal mol^{-1}) and this leads to an Arrhenius activation energy (E_a) of 0.51 kcal mol^{-1}. The inverse reaction seems unlikely, given the great activation energy required (55.31 kcal mol^{-1}). Of the compound methods, G2 and G2(MP2) find the C1 complex slightly more stable with respect to the TS (−0.42 kcal mol^{-1} for both), while G3 and CBS-4 MB give an opposite stability order, albeit by small amounts (0.96 and 1.77 kcal mol^{-1}, respectively). An accurate analysis of the single terms which contribute to determining the total electronic energy in the model chemistry scheme shows that the difference in stability between C1 and TS (states) is inverted in the steps which use a large atomic basis set with inclusion of diffuse functions, namely, 6–311 + G(d,p) and 6–31 + G(d) for G3 and 6–311 + G(3d2f2df,p) for CBS-4 MB. The changes in stability order can be attributed to geometric parameters. Single-point energy calculations with a larger basis set employing equilibrium geometries derived from a smaller basis set could not correspond exactly with the true geometrical minimum for the former, especially if the point of minimum lies on a flattened energy curve. Inclusion of ZPE correction leads to an inversion of stability, except in the case of 6–31 g *MP2(Full). This depends on the very small difference in the total electronic energies and on the energy values for the first vibrational state, which are very close but lower for the TS state. The calculated E_a values are very small or slightly negative. The activation energy values show that the reaction is much favoured, if not free and easy.

$$CH_3S^- + O_2 \rightleftarrows CH_3S^\cdot + O_2^{-\cdot}$$

Table 4. Molecular energy differences ΔE (without ZPE correction), $\Delta E(0)$ (with ZPE correction), and thermodynamic properties (ΔH, ΔG, and ΔS) for the reaction $^3O_2 \rightarrow {}^1O_2$

	ΔE^a	$\Delta E(0)^a$	ΔH^a	ΔG^a	ΔS^b
MP2(Full) /6–31G*					
$^3O_2$	0.00	0.00	0.00	0.00	0.00
$^1O_2$	35.05	34.78	34.78	35.40	−2.07
G2					
$^3O_2$	0.00	0.00	0.00	0.00	0.00
$^1O_2$	27.17	26.90	26.90	27.52	−2.07
G2(MP2)					
$^3O_2$	0.00	0.00	0.00	0.00	0.00
$^1O_2$	26.65	26.38	26.38	27.00	−2.07
G3					
$^3O_2$	0.00	0.00	0.00	0.00	0.00
$^1O_2$	29.53	29.26	29.26	29.88	−2.07
CBS-4 MB					
$^3O_2$	0.00	0.00	0.00	0.00	0.00
$^1O_2$	34.79	34.52	34.52	35.14	−2.07

[a] kcal mol^{-1}
[b] cal mol^{-1}

Table 5. Molecular energy differences ΔE (without ZPE correction), $\Delta E(0)$ (with ZPE correction), and thermodynamic properties (ΔH, ΔG, and ΔS) for the reaction $2CH_3S^\cdot \rightarrow CH_3SSCH_3$

	ΔE^a	$\Delta E(0)^a$	ΔH^a	ΔG^a	ΔS^b
MP2(Full)/6–31G*					
$CH_3S^\cdot + CH_3S^\cdot$	0.00	0.00	0.00	0.00	0.00
CH_3SSCH_3	−56.16	−52.55	−53.07	−40.80	−41.15
G2					
$CH_3S^\cdot + CH_3S^\cdot$	0.00	0.00	0.00	0.00	0.00
CH_3SSCH_3	−67.66	−64.05	−64.57	−52.30	−41.15
G2(MP2)					
$CH_3S^\cdot + CH_3S^\cdot$	0.00	0.00	0.00	0.00	0.00
CH_3SSCH_3	−69.59	−65.98	−66.50	−54.23	−41.15
G3					
$CH_3S^\cdot + CH_3S^\cdot$	0.00	0.00	0.00	0.00	0.00
CH_3SSCH_3	−66.17	−62.56	−63.08	−50.81	−41.15
CBS-4 MB					
$CH_3S^\cdot + CH_3S^\cdot$	0.00	0.00	0.00	0.00	0.00
CH_3SSCH_3	−66.69	−63.08	−63.60	−51.33	−41.15

[a] kcal mol^{-1}
[b] cal mol^{-1}

Table 6. Molecular energy differences ΔE (without ZPE correction), $\Delta E(0)$ (with ZPE correction), and thermodynamic properties (ΔH, ΔG, and ΔS) with respect to transition state for the reaction $CH_3SH + O_2^{-\cdot} \rightarrow CH_3S^{\cdot} + HO_2^{-}$. Arrhenius parameters ($E_a$, log k, and log A) at 298.15 K

	ΔE^a	$\Delta E(0)^a$	ΔH^a	ΔG^a	ΔS^b	E_a	log k^c	log A^c
MP2(Full)/6–31G*								
$CH_3SH + O_2^{-\cdot}$	22.01	21.65	22.21	14.54	25.71			
C1	−0.10	1.36	1.70	1.74	−0.14			
TS	0.00	0.00	0.00	0.00	0.00	−1.11	14.10	17.67
C2	−3.55	−2.08	−1.68	−2.71	3.45			
$CH_3S^{\cdot} + HO_2^{-}$	54.31	53.86	54.51	45.48	30.29			
G2								
$CH_3SH + O_2^{-\cdot}$	19.81	19.45	20.01	12.35	25.71			
C1	0.85	2.32	2.66	2.70	−0.14			
TS	0.00	0.00	0.00	0.00	0.00	−2.07	14.80	17.67
C2	−4.99	−3.52	−3.12	−4.15	3.45			
$CH_3S^{\cdot} + HO_2^{-}$	41.16	40.71	41.36	32.33	30.29			
G2(MP2								
$CH_3SH + O_2^{-\cdot}$	21.01	20.65	21.22	13.55	25.71			
C1	1.07	2.53	2.88	2.92	−0.14			
TS	0.00	0.00	0.00	0.00	0.00	−2.28	14.96	17.67
C2	−5.06	−3.59	−3.19	−4.22	3.45			
$CH_3S^{\cdot} + HO_2^{-}$	41.80	41.34	42.00	32.97	30.29			
G3								
$CH_3SH + O_2^{-\cdot}$	19.92	19.56	20.12	12.45	25.71			
C1	1.02	2.48	2.83	2.87	−0.14			
TS	0.00	0.00	0.00	0.00	0.00	−2.23	14.92	17.67
C2	−5.98	−4.51	−4.11	−5.14	3.45			
$CH_3S^{\cdot} + HO_2^{-}$	41.28	40.83	41.48	32.45	30.29			
CBS-4 MB								
$CH_3SH + O_2^{-\cdot}$	15.87	15.51	16.07	8.41	25.71			
C1	0.52	1.98	2.33	2.37	−0.14			
TS	0.00	0.00	0.00	0.00	0.00	−1.73	14.56	17.67
C2	−2.44	−0.97	−0.57	−1.60	3.45			
$CH_3S^{\cdot} + HO_2^{-}$	42.90	42.24	42.90	33.86	30.29			

[a] kcal mol^{-1}
[b] cal mol^{-1}
[c] cm^3 mol^{-1} s^{-1}

The reaction consists in an electron transfer from the thiolate anion to an oxygen molecule that yields the thiyl radical and a molecule of superoxide. At the MP2(Full)/6–31G* level a transition state TS was localised with a single imaginary frequency. IRC [27] analysis indicates the presence of two non-covalent intramolecular complexes along the reaction channels, namely, C1 (entrance channel) and C2 (leaving channel). TS, C1, and C2 belong to an electronic singlet state, whereas in the reagents the oxygen is a triplet and the products are both doublets. In order to achieve coherence in a spin multiplicity state, analysis of the course of the reaction must consider the oxygen molecule in the singlet state to be a reactant. A complete frequency analysis on C1 and C2 species confirms that these points are really minima in the reaction path and has enabled the thermal corrections to be determined (Table 3).

The geometrical structures of TS, C1, and C2 are reported in Fig. 2. In the entrance complex C1, the oxygen's atoms are equidistant from the sulfur atom and with the same net charge. The oxygen atoms increase their distance, but differently, from the sulfur atom in the TS state and charge polarisation takes place. The nearest oxygen exhibits a very small charge density, while the net charges of the farthest oxygen and the sulfur atom are smaller and greater, respectively, than in the complex C1. The sum of the net charge on the three atoms (two O and one S) are the same in all three molecular species (C1, TS, and C2). In the leaving complex C2, the distances of the oxygen atoms from the sulfur atom differ. The nearest oxygen again has a charge density nearly equal to that on the TS state, while the farthest oxygen shows a net increase in charge density corresponding to the decrease on the sulfur atom. Charge transfer from the sulfur atom of the thiolate anion to the oxygen molecule has taken place. This analysis of the reaction channel based on the geometrical and net charge behaviour seems to be satisfactory. But analysis of the behaviour of the energy along the reaction co-ordinate raises certain points for discussion. At MP2(Full)/6–31G* the entrance complex C1 is more stable than the transition state, as well as being of very low quantity. The introduction of the ZPE correction reverses the order of stability and this could be attributed to the same effects discussed for the previous reaction. The reaction would appear to be very ready with an activation energy of −1.38 kcal mol^{-1}. The energies obtained employing the compound methods raise a few doubts. According to the method employed, the complex C1 is found to be more unstable than the TS

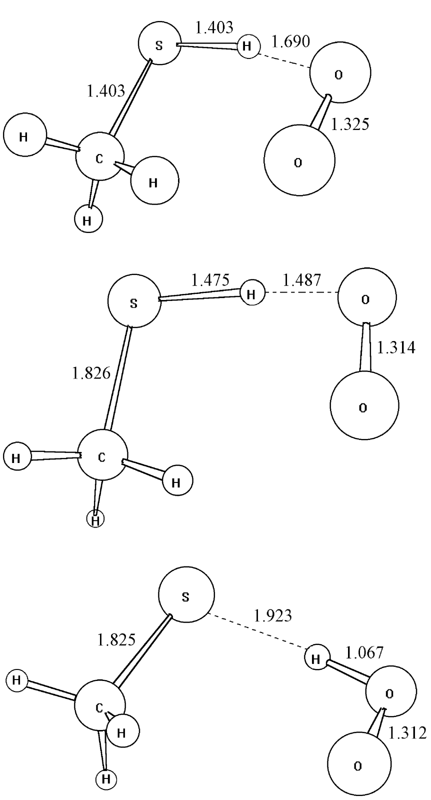

Fig. 3. Features of the optimized MP2(Full)/6-31G* geometries of C1, TS and C2 for Eq. (5). Distances in Å

by 2–7 kcal mol^{-1}. This could make one think that complex C1 might be an anomalous point on the reaction path when the path is studied with the compound methods, although it has all the characteristic features of an energy minimum at MP2(Full)/6–31G* level, which is the starting level for all the compound methods in order to determine equilibrium geometries and the nature (ground or transition state) of the molecular species. Besides, if it is assumed that the starting point for the energy behaviour in the reaction path is the sum of the reagent energies, without the inclusion of the ZPE correction, then for G2, G2(MP2), and G3 the complex C1 lies simply between the reactants and the TS. along the reaction co-ordinate, without being a characterized point. With the inclusion of the ZPE correction and in the CBS-4 MB scheme, C1 should be a point of maximum energy. This is in contrast with what was previously affirmed. The nature of this molecular non-covalent complex turns out to be very doubtful, also in view of the very poor stability found at MP2(Full)/6–31G*. The reaction scheme is based on the assumption that oxygen reacts as a singlet while its fundamental state is triplet. First, it is necessary that the oxygen be promoted from the fundamental triplet state to the excited singlet state. Table 4 reports the energies required, calculated at the different theory levels for this process. This step requires approximately 30 kcal mol^{-1}. The reaction then proceeds according to the previous scheme (C1 → TS → C2) with a small negative activation energy, but through the formation of a dubious C1 complex. Alternatively, the starting reactants could be the thiolate anion and the oxygen as triplet. This reaction starting point is more stable than that of the TS (Table 3) and the energy required for the reaction varies between 24 and 34 kcal mol^{-1}, depending on the method of calculation. This path requires no entrance complex and could be more likely. In any case, both for the first scheme (C1 → TS → C2) and for the second ($CH_3S^- + {}^3O_2 \rightarrow TS \rightarrow C2$) the energy required for the reaction is practically the same ($\sim$30 kcal mol^{-1}), with the second scheme slightly favoured.

$2CH_3S^{\cdot} \rightleftarrows CH_3SSCH_3$

The reaction is fundamentally the combination of two radicals and should be very fast without any activation energy. The dimerization is exothermic with an experimental heat of reaction of –65.4 kcal mol^{-1}. The compound methods yield values very close to the experimental one (Table 5), while the simplest MP2(Full)/6–31G* yields a value 12.33 kcal mol^{-1} lower. The formation of the disulfide species removes thiyl radicals from surrounding reactions and, consequently, shifts the equilibrium of the previous reactions towards the product reaction. The same observation applies to the subsequent reactions (Eqs. 5, 6, and 7) that lead to the formation of three other molecules of the thiyl radical.

$CH_3SH + O_2^{-\cdot} \rightleftarrows CH_3S^{\cdot} + HO_2^-$

The reaction consists in the extraction of an hydrogen atom by the superoxide ion. The values of Table 1 show the reaction to be endothermic, and it would appear to take part in determining the rate of the whole reaction (Eq. 1). Table 6 shows the results of the calculations at the different levels and Fig. 3 the structures of the transition state and of the two complexes arranged in the entrance (C1) and leaving channels (C2). Transition state and complexes are characterized as described previously. For this reaction also MP2(Full)/6–31G* calculations find an entrance complex slightly more stable with respect to the transition state (−0.10 kcal mol^{-1}), although the inclusion of the ZPE correction or the compound methods reverse the order of stability. This can be explained by the same arguments previously put forward. The calculated activation energy (E_a) is very low and has a negative value. The reaction seems to proceed very fast and easily with the formation of a fairly stable leaving complex. The following breaking of the complex with the formation of the final products requires an energy input of around 45 kcal mol^{-1}. This energy requirement, rather than a high value of activation energy, seems to govern the course of the reaction.

$CH_3SH + HO_2^- \rightarrow CH_3S^{\cdot} + OH^- + OH^{\cdot}$

The hydroperoxyl anion, generated from the previous step (Eq. 5), abstracts an hydrogen atom from a thiol

Table 7. Molecular energy differences ΔE (without ZPE correction), $\Delta E(0)$ (with ZPE correction), and thermodynamic properties (ΔH, ΔG, and ΔS) with respect to transition state for the reaction $CH_3SH + HO_2^- \rightarrow CH_3S^{\cdot} + OH^- + OH^{\cdot}$. Arrhenius parameters ($E_a$, log k, and log A) at 298.15 K

	ΔE[a]	$\Delta E(0)$[a]	ΔH[a]	ΔG[a]	ΔS[b]	E_a	log k[c]	log A[c]
MP2(Full)/6–31G*								
$CH_3SH+HO_2^-$	25.64	24.58	25.23	14.99	34.33			
C1	−1.03	−0.56	−0.27	−1.01	2.50			
TS	0.00	0.00	0.00	0.00	0.00	0.86	16.46	39.35
C2	−37.12	−34.85	−34.52	−36.00	4.95			
$CH_3S^{\cdot}+OH^-+OH^{\cdot}$	71.42	66.17	68.27	49.37	63.39			
G2								
$CH_3SH+HO_2^-$	17.75	16.69	17.34	7.11	34.33			
C1	0.47	0.94	1.22	0.48	2.50			
TS	0.00	0.00	0.00	0.00	0.00	−0.63	17.55	39.35
C2	−28.13	−25.86	−25.53	−27.00	4.95			
$CH_3S^{\cdot}+OH^-+OH^{\cdot}$	52.96	47.70	49.81	30.90	63.39			
G2(MP2)								
$CH_3SH+HO_2^-$	17.92	16.86	17.51	7.28	34.33			
C1	0.50	0.97	1.25	0.51	2.50			
TS	0.00	0.00	0.00	0.00	0.00	−0.66	17.57	39.5
C2	−28.55	−26.28	−25.94	−27.42	4.95			
$CH_3S^{\cdot}+OH^-+OH^{\cdot}$	53.58	48.32	50.43	31.53	63.39			
G3								
$CH_3SH+HO_2^-$	17.72	16.66	17.31	7.08	34.33			
C1	0.45	0.92	1.20	0.46	2.50			
TS	0.00	0.00	0.00	0.00	0.00	−0.61	17.54	17.54
C2	−29.60	−27.33	−27.00	−28.47	4.95			
$CH_3S^{\cdot}+OH^-+OH^{\cdot}$	51.40	46.15	48.25	29.35	63.39			
CBS-4 MB								
$CH_3SH+HO_2^-$	15.50	14.44	15.09	4.85	34.34			
C1	0.85	1.32	1.61	0.86	2.50			
TS	0.00	0.00	0.00	0.00	0.00	−1.01	17.84	17.54
C2	−28.41	−26.14	−25.80	−27.28	4.95			
$CH_3S^{\cdot}+OH^-+OH^{\cdot}$	47.63	42.38	44.48	25.58	63.39			

[a] kcal mol^{-1}
[b] cal mol^{-1}
[c] $cm^3\ mol^{-1}\ s^{-1}$

molecule and leads to the formation of three molecular fragments: the thiyl radical (which can react according to Eq. (4)), an hydroxyl ion (which restores the basic catalyst) and an hydroxyl radical (involved in Eq. (7)). The reaction behaviour is very similar to that of the previous steps (Eqs. 3 and 5): formation of an entrance complex, slightly more or less stable than in the transition state, a transition state, and a fairly stable leaving complex. Table 7 reports the results of the calculations and Fig. 4 shows the geometrical features of the adducts of interest. The activation energy (E_a) is very low (−1.01 to 0.86 kcal mol^{-1}) and would suggest a very fast and easy process.

The structure of the leaving complex shows one molecule of hydrogen peroxide symmetrically bonded to the sulfur atom. The first breaking of this complex yields the formation of a thiyl radical and a molecule of hydrogen peroxide radical anion. The breaking of the O–O bond in the last molecule yields the hydroxyl anion and radical, which are thus available for the other steps (Eqs. 2 and 7). The behaviour of this bond dissociation has been previously studied [28] by the ab-initio MCSCF method. The hydrogen peroxide radical anion, generated by an adiabatic one-electron transfer to the hydrogen peroxide molecule, relaxes to an almost planar equilibrium geometry with one hydrogen atom shifted between the oxygen atoms. The O–O bond cleavage requires 36.15 kcal mol^{-1} and no transition state has been shown [28]. In the present study the breaking of the leaving complex with the formation of the hydroxyl anion and radical requires about 80 kcal mol^{-1}, depending on the method employed. For this step also it is the last process which determines the endothermic character of the reaction and not the hydrogen abstraction, which requires little or no activation energy.

$$CH_3SH + OH^{\cdot} \rightarrow CH_3S^{\cdot} + H_2O$$

This reaction has been widely studied both experimentally [29] and by theoretical chemistry [30] owing to its importance in the chemistry of the atmosphere. Kinetics studies [29] have found a negative dependence in the 244–430 K range for the rate constant with an E_a of -0.7 ± 0.2 kcal mol^{-1}. The hydrogen abstraction with the formation of a thiyl radical can be considered either as a separate reaction for the formation of a disulfide molecule or as a step in the mechanism of oxidation of sulfide compounds. Instead of hydrogen abstraction, the

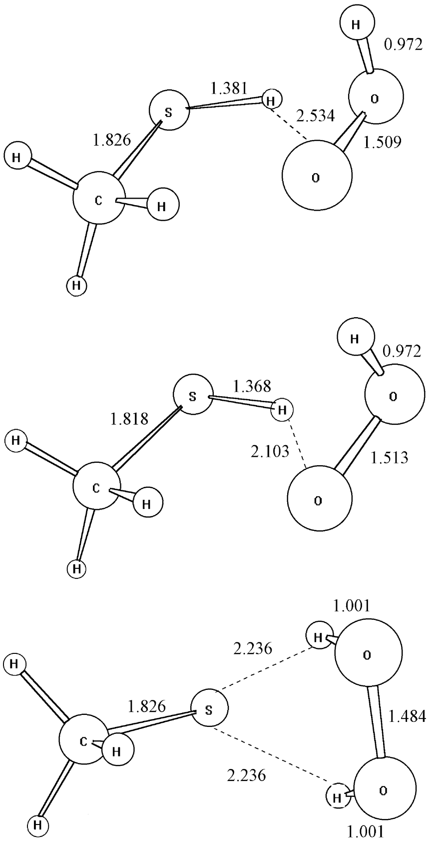

Fig. 4. Features of the optimized MP2(Full)/6-31G* geometries of C1, TS and C2 for Eq. (6). Distances in Å

reaction could proceed with the addition of the hydroxyl radical to the sulfide atom to form the oxygenated compound $CH_3S(OH)H$. The ab-initio study [30] has suggested that the formation of the oxygenated adduct is slightly endothermic (1.4 kcal mol^{-1}), whereas the abstraction reaction has no activation energy and is therefore the favourite. The authors concluded that the reaction proceeds via the extraction of the sulfur-bonded hydrogen. The calculated energy path, reported here, establishes the formation of two complexes (entrance and leaving channels) that are more stable than the transition state for any theoretical approach used. The minor values are for the compound methods. Calculated values are reported in Table 8 and geometrical features are depicted in Fig. 5. The calculated activation energy amounts to 7.60 kcal mol^{-1} at the MP2(Full)/6–31G* level and ranges between 1.31 and 1.63 kcal mol^{-1} for the compound methods. The latter values are not much higher than the experimental one but are of opposite sign. Previous theoretical calculations [30], which adopted a different scheme for the calculation of single corrective contributions to total electronic energy, found better agreement with regard to both value (−0.64 kcal mol^{-1}) and sign. In this analysis of the channel of reaction the authors did not consider the possibility of the intermediate complexes forming, and the E_a value was determined as the difference between the energy of the transition state and that of the two isolated reactants. Using the present approach, new values for E_a have been calculated and are reported in parentheses in Table 8. Except for the MP2(Full)/6–31G* approach, which again yields a positive value (4.94 kcal mol^{-1}), the compound methods yield a small negative value (−1.56–0.86 kcal mol^{-1}) very close to the experimental one (-0.7 ± 0.2 kcal mol^{-1}). This result could raise a doubt as to whether the Van der Waals complexes are a real species or merely an artifice of the calculation. This doubt is plausible because, for instance, the distance between the two reagent molecules in the complex is quite large. Analysis of the geometrical features in the complexes shows, however, that the bonded molecules are very similar in structure to the isolated molecule but are orientated in such a way as to explain the course of reaction. For this reaction, the oxygen atom of the hydroxyl radical points to hydrogen bonded to the sulfur atom. In the transition state the O–H distance diminishes when the S–H distance lengthens. The leaving complex displays a lengthening of the S–distance (breaking bond) and a simultaneous shortening of the O–H bond (forming bond) with the formation of a water molecule. The whole description is in agreement with the mechanism of hydrogen abstraction and serves to

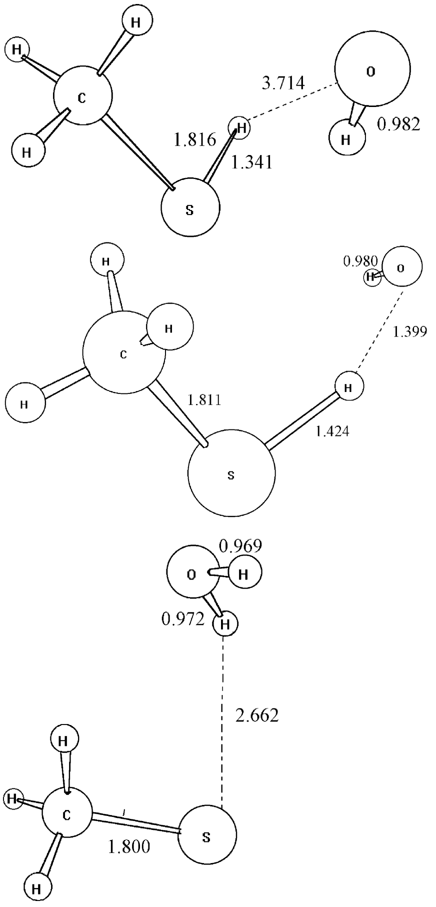

Fig. 5. Features of the optimized MP2(Full)/6-31G* geometries of C1, TS and C2 for Eq. (7). Distances in Å

Table 8. Molecular energy differences ΔE (without ZPE correction), $\Delta E(0)$ (with ZPE correction), and thermodynamic properties (ΔH, ΔG, and ΔS with respect to transition state for the reaction $CH_3SH + OH^{\cdot} \rightarrow CH_3S^{\cdot} + H_2O$. Arrhenius parameters ($E_a$, log k, and log A) at 298.15 K

	ΔE[a]	$\Delta E(0)$[a]	ΔH[a]	ΔG[a]	ΔS[b]	E_a	log k[c]	log A[c]
MP2(Full)/6–31G*								
$CH_3SH + OH^{\cdot}$	−5.27	−5.11	−4.35	−12.44	27.13			
C1	−9.11	−7.61	−7.01	−9.68	8.95			
TS	0.00	0.00	0.00	0.00	0.00	7.60	10.65	16.22
C2	−43.08	−39.70	−38.98	−40.79	6.06	(4.94	8.63	12.25)[d]
$CH_3S^{\cdot} + H_2O$	−39.17	−37.70	−36.90	−45.53	28.97			
G2								
$CH_3SH + OH^{\cdot}$	1.30	1.46	2.22	−5.87	27.13			
C1	−2.82	−1.32	−0.72	−3.39	8.95			
TS	0.00	0.00	0.00	0.00	0.00	1.31	15.26	16.22
C2	−36.03	−32.65	−31.94	−33.75	6.06	(−1.62	13.44	12.25)[d]
$CH_3S^{\cdot} + H_2O$	−32.22	−30.75	−29.95	−38.59	28.97			
G2 (MP2)								
$CH_3SH + OH^{\cdot}$	1.24	1.40	2.15	−5.93	27.13			
C1	−2.89	−1.39	−0.79	−3.46	8.95			
TS	0.00	0.00	0.00	0.00	0.00	1.39	15.21	16.22
C2	−36.04	−32.67	−31.95	−33.76	6.06	(−1.56	13.44	12.25)[d]
$CH_3S^{\cdot} + H_2O$	−32.29	−30.82	−30.02	−38.66	28.97			
G3								
$CH_3SH + OH^{\cdot}$	1.33	1.49	2.25	−5.84	27.13			
C1	−2.83	−1.33	−0.73	−3.40	8.95			
TS	0.00	0.00	0.00	0.00	0.00	1.33	15.25	16.22
C2	−35.79	−32.41	−31.70	−33.51	6.06	(−1.65	13.46	12.25)[d]
$CH_3S^{\cdot} + H_2O$	−32.04	−30.57	−29.77	−38.41	28.97			
CBS-4 MB								
$CH_3SH + OH^{\cdot}$	0.54	0.70	1.46	−6.63	27.13			
C1	−3.13	−1.64	−1.04	−3.71	8.95			
TS	0.00	0.00	0.00	0.00	0.00	1.63	15.03	16.22
C2	−36.00	−32.62	−31.91	−33.72	6.06	(−0.86	12.89	12.25)[d]
$CH_3S^{\cdot} + H_2O$	−32.41	−30.94	−38.77	−38.77	28.97			

[a] kcal mol^{-1}
[b] cal mol^{-1}
[c] cm^3 mol^{-1} s^{-1}
[d] Without considering the formation of complex C1

support the formation of intermediate complexes. The IRC analysis indicates the formation of complexes.

In conclusion, the reactions have very low energy requirements and should be very fast and easy.

4. Conclusion

The analysis of each single step of the reactions allows a number of conclusions to be drawn. The exothermic reactions (Eqs. 2, 4, and 7) require little activation energy and should occur easily with a slight influence on the rate of the whole reaction (Eq. 1). The contribution of the endothermic reactions is more intricate. For the reaction depicted by Eq. (3) the charge transfer process, (whether considering the formation of an entrance complex or considering the two separate reactants as starting point) is very fast with a negative activation energy value. The greater energy requirement is due either to the transition of the oxygen atom from a triplet electronic state to a singlet state or to direct derivation of the transition state starting from the oxygen triplet. Both processes require about 30 kcal mol^{-1}. Later, the breaking of the leaving complex to yield the final products requires again about 30 kcal mol^{-1}. The reactions depicted by Eqs. (5) and (6) show very similar behaviour. Both require for the formation of the leaving complex a negative value of activation energy and predict a very fast process. The second step, the breaking of the complex with the formation of the final products, requires a very high energy contribution of 45–80 kcal mol^{-1}. The products formed in the reactions depicted by Eqs. (5) and (6) are the reagents for the other steps. This could help the course of that reaction. It seems that it is not the activation energy for the reaction but the following breaking reaction forming the final products that governs the rate of the reaction and determines the endothermic character of the step.

With regard to methods of calculation, the results obtained show that the simplest method used (MP2(Full)/6–31G*) affords a good description of the reaction pathway but with higher activation energy values than those obtained by other methods and also higher than whatever experimental values are available. It is the least reliable for quantitative analysis of both activation energy and enthalpies of reaction. The enthalpies of reaction are well reproduced by the compound methods with a very small error for the global reaction (Eq. 1) and a slightly higher value for any single step. The CBS-4 MB method, which is the one requiring the least calculation resources, works rather well. Of all the methods, G3 is the one that works best and provides the fewest errors. The compound methods prove to be very useful in the study of reaction kinetics but must be used with care if very low energy barriers are being studied. The use of a very large basis set to determine corrections to total electronic energy would create a few uncertainties regarding the localization of characterized points (for instance, minima and transition states). This could depend on the fact that the geometrical parameters used in the calculations correspond to an energy minimum for another, lesser basis set. For the higher basis set, the energy minimum could have shifted and therefore no longer be the true minimum. This shift, even if very small, can exert an influence on the determination of very small energy values.

Acknowledgements. Financial support from the Ministero per l'Università e la Ricerca Scientifica and computing facilities from the Centro di Calcolo Interuniversitario dell'Italia Nord Orientale and from the Centro di Calcolo dell'Università di Modena e Reggio Emilia are warmly acknowledged.

References

1. Beck-Speier I, Leuschel L, Luippold G, Maier KL (1988) FEBS Lett 227:1–4
2. Vogt W (1995) Free Radical Biol Med 18:93–105
3. Capaldo K, Corbett JJ, Kasibhatla P, Fischbeck P, Pandis SN (1999) Nature 400:743–746
4. Bahenemann D (1990) In: Chatgilialoglu C, Asmus K-D (eds) Sulfur-centered reactive intermediates in chemistry and biology, NATO ASI Series 197. Plenum Press, New York, pp 103–120
5. Stryer L (1988) Biochemistry, 3rd edn. Freeman, New York
6. Osvald AA, Wallace TJ (1966) In: Kharasch N, Meyers CY (eds) The chemistry of organic sulfur compounds, vol 2. Pergamon Press, New York
7. Ohno A, Oae S (1977) In: Oae S (ed) Organic chemistry of sulfur. Plenum Press, New York
8. Chen CJ, Bozzelli JW (2000) J Am Chem Soc 104:4997–5012
9. Yamada T, Bozzelli JW, Lay TH (2000) Int J Chem Kinet 32:435–452
10. Chen CJ, Bozzelli JW (2000) J Phys Chem A 104:9715–9732
11. Somnitz H, Zellner R (2000) Phys Chem Chem Phys 2:1899–1905
12. Frisch MJ, Trucks GW, Schlegel HB, Gill PMW, Johnson BG, Robb MA, Cheeseman JR, Keith T, Petersson GA, Montgomery JA, Raghavachari K, Al-Laham MA, Zakrzewski VG, Ortiz JV, Foresman JB, Cioslowski J, Stefanov BB, Nanayakkara A, Challacombe M, Peng CY, Ayala PY, Chen W, Wong MW, Andres JL, Replogle ES, Gomperts R, Martin RL, Fox DJ, Binkley JS, Defrees DJ, Baker J, Stewart JP, Head-Gordon M, Gonzalez C, Pople JA (1995) Gaussian 94 Revision D3. Gaussian Inc, Pittsburgh, PA
13. Frisch MJ, Trucks GW, Schlegel HB, Scuseria GE, Robb MA, Cheeseman JR, Zakrzewski VG, Montgomery JA Jr, Stratmann RE, Burant JC, Dapprich S, Millam JM, Daniels AD, Kudin KN, Strain M, Farkas CO, Tomasi J, Barone V, Cossi M, Cammi R, Mennucci B, Pomelli C, Adamo C, Clifford S, Ochterski J, Petersson GA, Ayala P, Cui YQ, Morokuma KD, Malick K, Rabuck AD, Raghavachari K, Foresman JB, Cioslowski J, Ortiz JV, Baboul AG, Stefanov BB, Liu G, Liashenko A, Piskorz P, Komaromi I, Gomperts R, Martin LR, Fox DJ, Keith T, Al-Laham MA, Peng CY, Nanayakkara A, Gonzalez C, Challacombe M, Gill PMW, Johnson B, Chen W, Wong MW, Andres JL, Gonzalez C, Head-Gordon M, Replogle ES, Pople JA (1998) Gaussian 98 revision,7. Gaussian Inc, Pittsburgh, PA
14. Montgomery JA Jr, Frisch MJ, Ochterski JW, Petersson GA (2000) J Chem Phys 112:6532
15. Benassi R, Taddei F (2000) J Comput Chem 21:1405; Benassi R (2001)Theor Chem Acc 106:259–263
16. Curtiss LA, Raghavachari K, Trucks GW, Pople JA (1991) J Chem Phys 94:7221
17. Curtiss LA, Raghavachari K, Pople JA (1993) J Chem Phys 98:1293
18. Curtiss LA, Raghavachari K, Redfren PC, Rassolov V, Pople JA (1998) J Chem Phys 109:7764; Curtiss LA, Redfren PC, Raghavachari K, Rassolov V, Pople JA (1998) J Chem Phys 110:7764; Baboul AG, Curtiss LA, Redfren PC, Raghavachari K (1999) J Chem Phys 110:7650, Curtiss LA, Redfren PC, Raghavachari K, Pople JA (1999) Chem Phys Lett 313:600
19. Steinfeld JI, Franciso JS, Hase WL (1989) Chemical kinetics and dynamics. Prentice Hall, New York
20. Wigner EP (1932) Z Phys Chem B19:203
21. Chase MW Jr, Davies CA, Doweney JR Jr, Frurip DJ, McDonald RA, Syverd NJ (1985) J Phys Chem Reference Data 14, Suppl 1; Mallard WG Linstrom PJ (1998) In: NIST Chemistry WebBook, Natl Inst Stand Technol, MD
22. Nicolaides A, Radom L (1996) Mol Phys 88:759
23. Stewart R (1987) The proton: applications to organic chemistry. Academic Press, New York
24. Zahradník R, Hess BA Jr (1991) J Mol Struct (Theochem) 230:387
25. Cao HZ, Allavena M, Tapia O, Evleth EM (1985) J Phys Chem 89:1581
26. Benassi R, Fiandri LG, Taddei F (1995) J Org Chem 60:5855
27. Gonzalez C, Schlegel HB (1989) J Chem Phys 90:2154; Gonzalez C, Schlegel HB (1990) J Phys Chem 94:5523
28. Benassi R, Taddei F (1993) Chem Phys Lett 204:595
29. Tyndall GS, Ravishankara AR (1991) J Chem Kinet 23:83
30. Wilson C, Hirst DM (1995) J Chem Soc Faraday Trans 91:3783–3785